RadioGraphics

Hypertrophic Cardiomyopathy: Assessment with MR Imaging and Multidetector CT[1]

Eun Ju Chun, MD • Sang Il Choi, MD • Kwang Nam Jin, MD • Hyon Joo Kwag, MD • Young Jin Kim, MD • Byoung Wook Choi, MD • Whal Lee, MD Jae Hyung Park, MD

CME FEATURE

See www.rsna.org/education/rg_cme.html

LEARNING OBJECTIVES FOR TEST 4

After reading this article and taking the test, the reader will be able to:

- Identify the features and classify the phenotypes of hypertrophic cardiomyopathy (HCM) with MR imaging and multidetector CT.
- Discuss the potential role of MR imaging and multidetector CT in the assessment of HCM.
- List the risk factors involved with risk stratification of HCM, and guide proper management of HCM.

TEACHING POINTS

See last page

Hypertrophic cardiomyopathy (HCM) is a genetic cardiac disease. Its early detection is important because it is the most common cause of sudden cardiac death among young people. However, HCM is often a dilemma for clinicians because it manifests with diverse phenotypic expressions and clinical courses. With the advances in imaging technology, magnetic resonance (MR) imaging and multidetector computed tomography (CT) serve as suitable modalities for detecting and characterizing HCM and obtaining information for appropriate management of cases of HCM, although echocardiography is currently the most widely used modality. This article is an overview of the definition of HCM, its various phenotypes, risk stratification of HCM, and the potential application of cardiac MR imaging and multidetector CT for the assessment of HCM.

Abbreviations: DE = delayed enhancement, HCM = hypertrophic cardiomyopathy, LV = left ventricular, LVOT = left ventricular outflow tract

RadioGraphics 2010; 30:1309–1328 • **Published online** 10.1148/rg.305095074 • **Content Codes:** CA CT MR

[1]From the Division of Cardiovascular Imaging, Department of Radiology, Seoul National University Bundang Hospital, 300 Gumi-dong, Bundang-gu, Seongnam-si, Gyeonggi-do 436-707, Korea (E.J.C., S.I.C., K.N.J.); Department of Radiology, Kangbuk Samsung Hospital, Sungkyunkwan University College of Medicine, Seoul, Korea (H.J.K.); Department of Radiology and Research Institute of Radiological Science, Severance Hospital, Yonsei University College of Medicine, Seoul, Korea (Y.J.K., B.W.C.); and Department of Radiology and Institute of Radiation Medicine, Seoul National University College of Medicine, Clinical Research Institute, Seoul National University Hospital, Seoul, Korea (W.L., J.H.P.). Recipient of a Cum Laude award for an education exhibit at the 2008 RSNA Annual Meeting. Received April 1, 2009; revision requested June 22 and received April 14, 2010; accepted April 20. For this CME activity, the authors, editors, and reviewers have no relevant relationships to disclose. **Address correspondence to** S.I.C. (e-mail: *drsic@radiol.snu.ac.kr*).

Introduction

Hypertrophic cardiomyopathy (HCM) is defined as a diffuse or segmental left ventricular (LV) hypertrophy with a nondilated and hyperdynamic chamber, in the absence of another cardiac or systemic disease capable of producing the magnitude of hypertrophy that is evident (1,2). HCM is inherited as a mendelian autosomal dominant trait and is caused by mutations in one of the sarcomeric genes, each of which encodes protein components of the cardiac sarcomeres, which are composed of thick or thin filaments (1). The pathologic hallmarks of HCM are myocyte disarray and interstitial fibrosis (3). Abnormal dysplasia of small intramural coronary arterioles is another common histopathologic finding, which is caused by increased pressure from adjacent hypertrophic myocytes (4).

Because the clinical manifestations and electrocardiographic findings are nonspecific and diverse, noninvasive imaging modalities play a pivotal role in detecting HCM and understanding its pathophysiology (5). The goals of noninvasive imaging in the evaluation of HCM are to distinctly diagnose the disease and characterize its phenotype, to assess cardiac function (including the presence of dynamic obstruction), to classify the disease severity and provide risk stratification, and to serve as a screening tool for the family and as a guide for appropriate therapy (1,2,5).

Echocardiography is the usual modality used as a screening procedure in the diagnosis and evaluation of LV hypertrophy; however, some limitations of the technique impede accurate diagnosis. Teaching Point Echocardiography is an operator-dependent technique. It is influenced by the acoustic window and is sometimes unable to definitively depict the endocardial border, especially the anterolateral free wall of the left ventricle in the parasternal short-axis view and the apex (2,6). The degree of LV hypertrophy could be underestimated by using echocardiography, and this underestimation, in fact, can delay proper treatment, thereby failing to prevent a sudden cardiac death (5).

On the contrary, cardiac magnetic resonance (MR) imaging is less dependent on the operator and is not subject to acoustic window limitations. Cine MR imaging with the steady-state free precession pulse sequence can offer the advantages of multiplanar imaging, complete coverage of the entire myocardium without obliquity, and excellent soft-tissue contrast between the myocardial border and the blood pool (7,8). Thus, cardiac MR imaging can allow better characterization of the pattern and distribution of LV hypertrophy in HCM. In addition, the status of myocardial blood flow can be assessed by using adenosine stress cardiac MR imaging. Delayed enhancement (DE) MR imaging techniques can provide unique information for tissue characterization, specifically for the identification of myocardial fibrosis or scarring (9,10).

Cardiac multidetector computed tomography (CT) has also emerged as a novel modality for evaluating cardiac morphology and function, as well as the coronary artery. In comparison with the spatial resolution of MR imaging, the spatial resolution of multidetector CT is usually higher, which enables high-quality multiplanar reconstructions in any desired image orientation, including three-dimensional reformatted images (11). Therefore, cardiac multidetector CT can offer *(a)* comprehensive information that includes detailed anatomic and functional information about the cardiac chambers and *(b)* high-quality noninvasive coronary angiography (12,13).

Teaching Point In a clinical setting for evaluation of HCM, although echocardiography is the simplest imaging technique to use for screening, cardiac MR imaging should be considered as the reference standard for establishing a diagnosis of HCM when the results from echocardiography are inconclusive or are suspected of being false-negative findings. Moreover, cardiac MR imaging is strongly recommended as a powerful imaging modality for differentiating HCM from other cardiomyopathies in the differential diagnosis, as well as for risk stratification of HCM in selected patients. In comparison, cardiac multidetector CT is certainly less useful for the assessment of HCM currently because multidetector CT involves radiation exposure and contrast medium–related problems and provides less information (ie, hemodynamic information, tissue characterization such as fibrosis) than MR imaging does. Although MR imaging and echocardiography may be the imaging modalities of choice in most cases of HCM, multidetector CT would be more appropriate in those cases for which there are specific requests to exclude coronary artery disease and in those cases with contraindications for MR imaging, such as a pacemaker (14).

The purpose of this article is to provide an overview of HCM by considering the roles of cardiac MR imaging and multidetector CT in comparison with echocardiography, with an emphasis on the phenotypes and risk stratification of HCM. The phenotypes of HCM that are

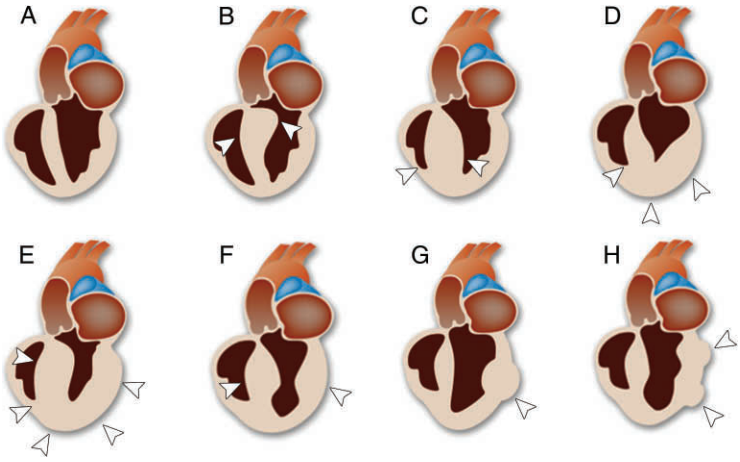

Figure 1. Drawings of the normal heart and the heart in the various phenotypes of HCM. The diagnostic criterion of HCM is that the maximal LV wall thickness is greater than or equal to 15 mm in the end-diastolic phase. *A,* Normal heart; *B,* asymmetric (septal) HCM with LVOT obstruction; *C,* asymmetric (septal) HCM without LVOT obstruction; *D,* apical HCM; *E,* symmetric HCM (concentric HCM); *F,* midventricular HCM; *G,* masslike HCM; *H,* noncontiguous HCM. The drawings of the various phenotypes of HCM show the areas of hypertrophy (arrowheads).

covered are asymmetric (septal) HCM, apical HCM, symmetric HCM (concentric HCM), midventricular HCM, masslike HCM, noncontiguous HCM, reverse-curve HCM and sigmoid HCM, and preclinical HCM. The criteria for risk stratification of HCM include LV wall thickness, left ventricular outflow tract (LVOT) obstruction, LV dilatation with depressed ejection fraction (burned-out phase), the presence of fibrosis, and perfusion defect.

Phenotypes of HCM

The rate of occurrence of HCM is about 0.2%, and HCM is a particularly common cause of sudden cardiac death in young people (2). Clinically, patients may be asymptomatic or may present with a wide variety of symptoms, including dyspnea, chest pain, syncope, or sudden cardiac death. Dyspnea on exertion is the most common symptom because the key functional hallmark of HCM is an impaired diastolic function with impaired LV filling in the presence of preserved systolic function (15). Systolic dysfunction often develops with end-stage HCM.

The usual diagnostic criterion for HCM is a maximal LV wall thickness greater than or equal to 15 mm in the end-diastolic phase. The morphologic expression of HCM is widely variable and heterogeneous because HCM may affect any portion of the left ventricle (16,17). Asymmetric (septal) involvement with HCM is the most common form of the disease, and other variants include apical, symmetric, midventricular, masslike, and noncontiguous HCM (18,19) (Fig 1).

Asymmetric (Septal) HCM

Asymmetric involvement of the interventricular septum is the most common form of the disease, accounting for an estimated 60%–70% of the cases of HCM (1). Asymmetric (septal) HCM is diagnosed when the septal thickness is greater than or equal to 15 mm or when the ratio of the septal thickness to the thickness of the inferior wall of the left ventricle is greater than 1.5 at the midventricular level (20). The hypertrophy in this phenotype of HCM is usually asymmetric and is typically most evident in the anteroseptal myocardium.

It is clinically important to distinguish between the obstructive and nonobstructive forms of HCM, on the basis of the presence or absence of a gradient between the LVOT and the aorta with the patient at rest and/or with provocation (1). Approximately 20%–30% of the patients with asymmetric (septal) HCM have a resting systolic pressure gradient of the LVOT caused by systolic anterior motion of the mitral valve leaflets and midsystolic contact with the interventricular septum (21). Concomitant mitral regurgitation is also frequently noted as a result of systolic anterior motion and incomplete leaflet apposition. Although the mechanism of systolic anterior motion remains unclear, a widely accepted explanation of this phenomenon is that raised flow velocities in an LVOT anatomically distorted by septal hypertrophy create a Venturi effect, pulling the mitral valve leaflets toward the septum and obstructing the outflow tract (22). Systolic anterior motion is not pathognomonic of HCM because systolic anterior motion may occur in patients with a hypertensive heart, diabetes mellitus, acute myocardial infarction, or mitral valve repair or dysfunction (23).

Cine cardiac MR imaging clearly demonstrates *(a)* systolic anterior motion of the mitral leaflets and *(b)* a high-velocity jet depicted as an area of high signal intensity or signal void within

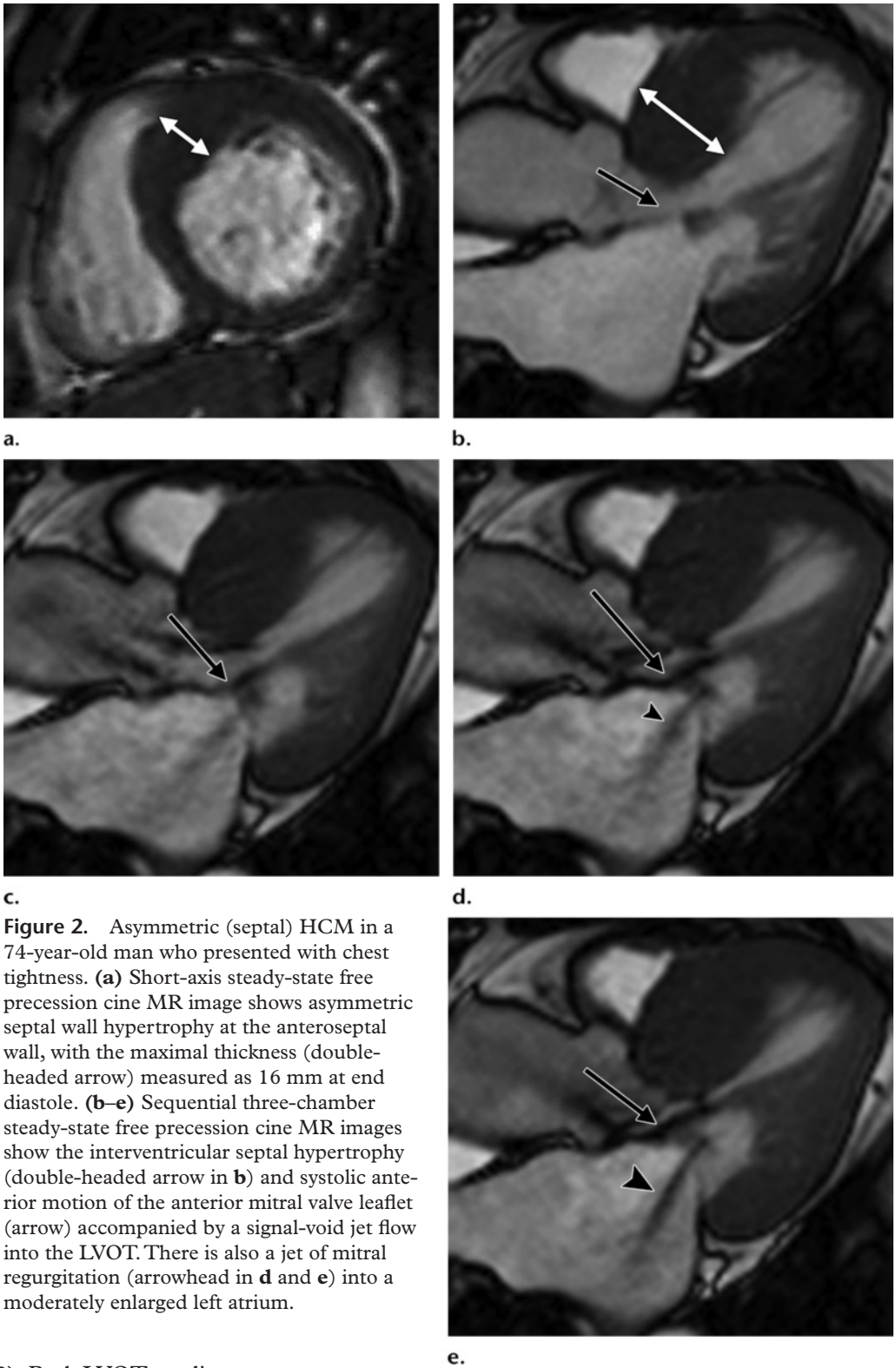

Figure 2. Asymmetric (septal) HCM in a 74-year-old man who presented with chest tightness. **(a)** Short-axis steady-state free precession cine MR image shows asymmetric septal wall hypertrophy at the anteroseptal wall, with the maximal thickness (double-headed arrow) measured as 16 mm at end diastole. **(b–e)** Sequential three-chamber steady-state free precession cine MR images show the interventricular septal hypertrophy (double-headed arrow in **b**) and systolic anterior motion of the anterior mitral valve leaflet (arrow) accompanied by a signal-void jet flow into the LVOT. There is also a jet of mitral regurgitation (arrowhead in **d** and **e**) into a moderately enlarged left atrium.

the LVOT (Fig 2). Peak LVOT gradients can be estimated by using phase-contrast MR imaging. However, these gradients are better assessed currently with echocardiography because of its higher temporal resolution when measuring peak instantaneous velocities (18). Cardiac multidetector CT can be used to assess the LVOT diameter and the presence of systolic anterior motion with multiphase images (Fig 3), although multidetector CT does not allow measurement of the LVOT gradient (24). However, some patients without

Figure 3. Asymmetric (septal) HCM with systolic anterior motion in a 44-year-old man who presented with dyspnea. **(a, b)** Three-chamber transthoracic echocardiograms obtained in the diastolic phase **(a)** and end-systolic phase **(b)** show anterior displacement of the anterior mitral leaflet (arrow) in the systolic phase. **(c, d)** Three-chamber multidetector CT images obtained in the diastolic phase **(c)** and end-systolic phase **(d)** demonstrate LV hypertrophy (double-headed arrow), with a thickened anterior mitral leaflet (arrow). Note the anterior motion of the mitral leaflet (arrow in **d**) in the systolic phase, which causes LVOT obstruction. **(e)** Short-axis multidetector CT image obtained in diastole clearly demonstrates asymmetric septal wall hypertrophy (double-headed arrow) at the anteroseptal wall, with an engorged septal branch (arrow).

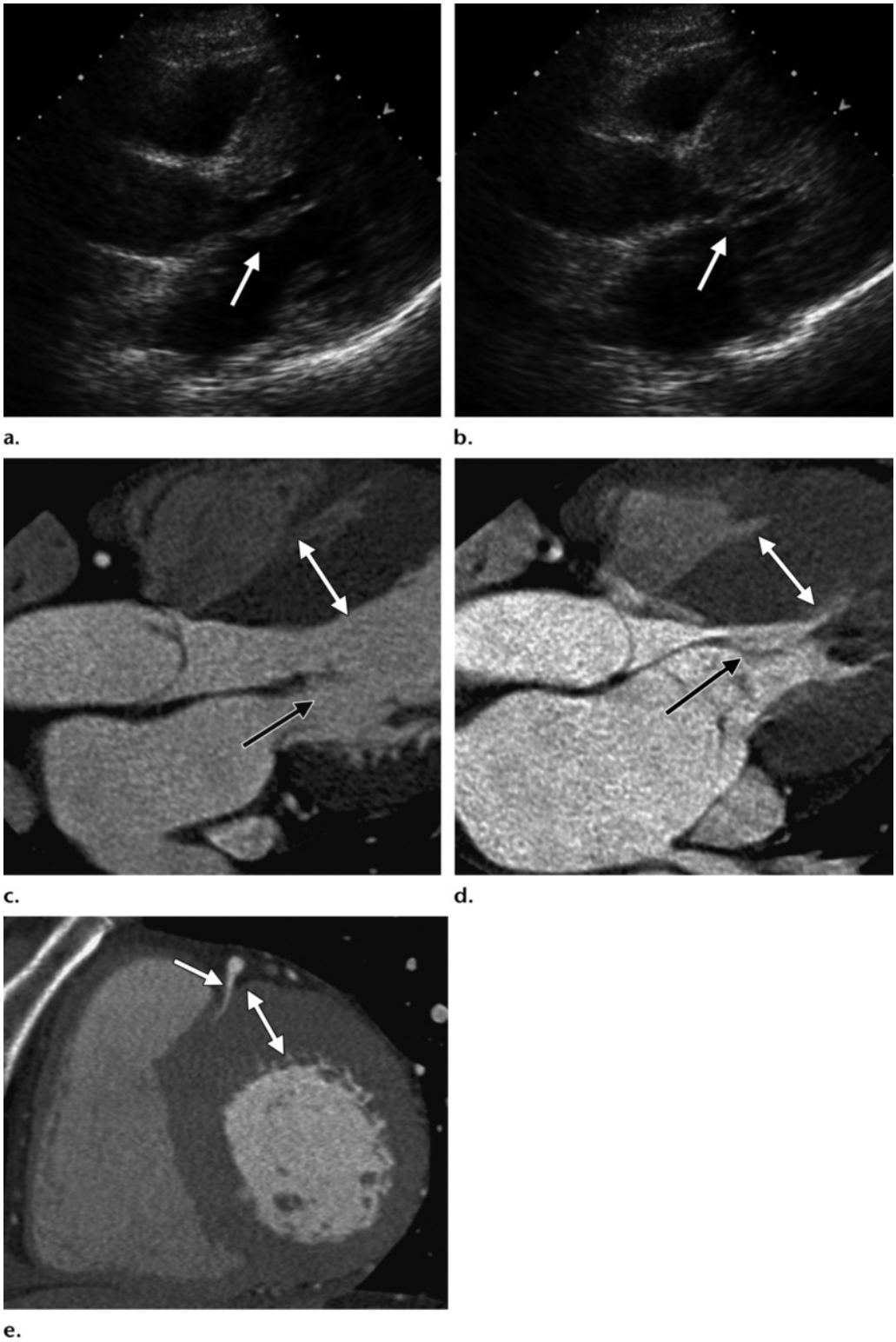

Figure 4. Asymmetric (septal) HCM with LVOT obstruction in a 74-year-old man who was treated with septal alcohol ablation. **(a)** Sequential four-chamber steady-state free precession cine MR images show the progression of wall thinning (arrowheads) that is due to the infarction after alcohol ablation at the basal interventricular septum. **(b)** Sequential four-chamber DE MR images show the infarcted myocardium in the corresponding areas (arrowheads).

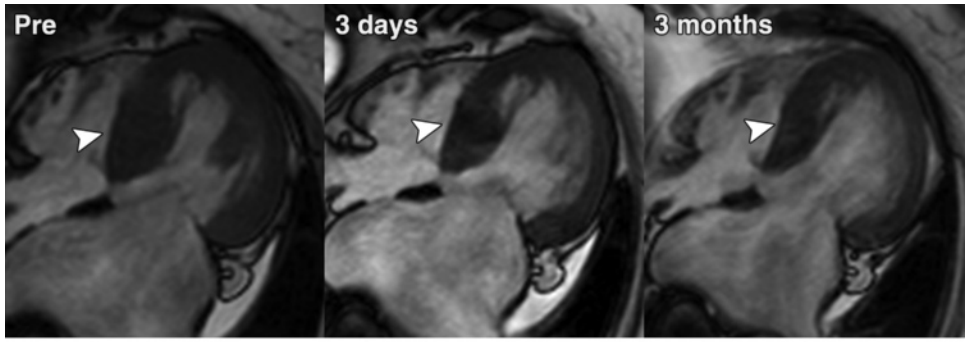

a.

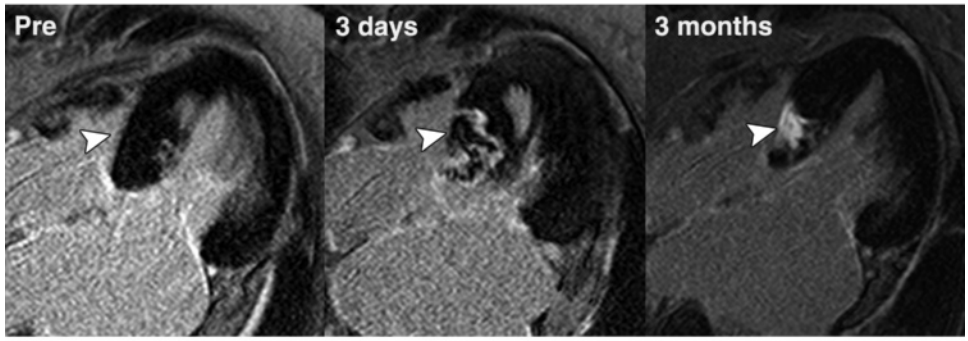

b.

LVOT obstruction at rest have systolic pressure gradients that can be provoked by using physiologic and pharmacologic interventions. This observation implies that LVOT obstruction may occur with spontaneous variability (labile obstruction) or with provocation by using pharmacologic or physiologic methods (latent obstruction). Approximately two-thirds of the patients with symptomatic nonobstructive HCM have latent LVOT obstruction (22). These patients should receive more vigorous therapy than those without latent obstruction (25). Therefore, the absence of systolic anterior motion at MR imaging and/or multidetector CT imaging cannot be interpreted as insignificant LVOT obstruction.

Medical treatment lessens the symptoms of heart failure but has not been shown to modify the clinical course. Patients with LVOT obstruction and severe symptoms unresponsive to medical therapy represent about 5% of the patients with HCM and are candidates for surgical myectomy or septal alcohol ablation, to be relieved of the LVOT obstruction (15). Patients with a dynamic obstruction (peak instantaneous gradient ≥50 mm Hg at rest or with provocation) or a septal thickness of more than 1.6 cm should be considered for septal reduction therapy such as septal myectomy or septal alcohol ablation (1). Septal myectomy is surgical resection of the hypertrophic segment of the interventricular septum. The procedure has an initial success rate of 90% in decreasing symptoms and LVOT obstruction; in about 70% of the patients, the lessening of symptoms is maintained (1,2). Septal alcohol ablation has been used as a nonsurgical procedure for iatrogenic infarction of the basal interventricular septum. MR imaging can be used to guide the determination of the exact extent and localization of septal hypertrophy for surgical reduction (26) and to monitor the remnant obstruction, the area of infarction of the septum, and the functional and morphologic changes, such as those in the LVOT gradient, the septal thickness, and the left atrial dimensions, after myectomy or septal alcohol ablation (27) (Fig 4).

Figure 5. Apical HCM in a 45-year-old man with electrocardiographic abnormalities that included QRS voltages associated with LV hypertrophy and giant negative T waves in leads V_5 and V_6. **(a)** Four-chamber transthoracic echocardiogram does not exactly define the apical endocardial border. **(b)** Four-chamber steady-state free precession cine MR image makes the apical endocardial border (arrows) clear. **(c)** Two-chamber steady-state free precession cine MR image shows apical hypertrophy (arrows) and obliteration of the LV apical cavity at end diastole, with a typical spadelike configuration.

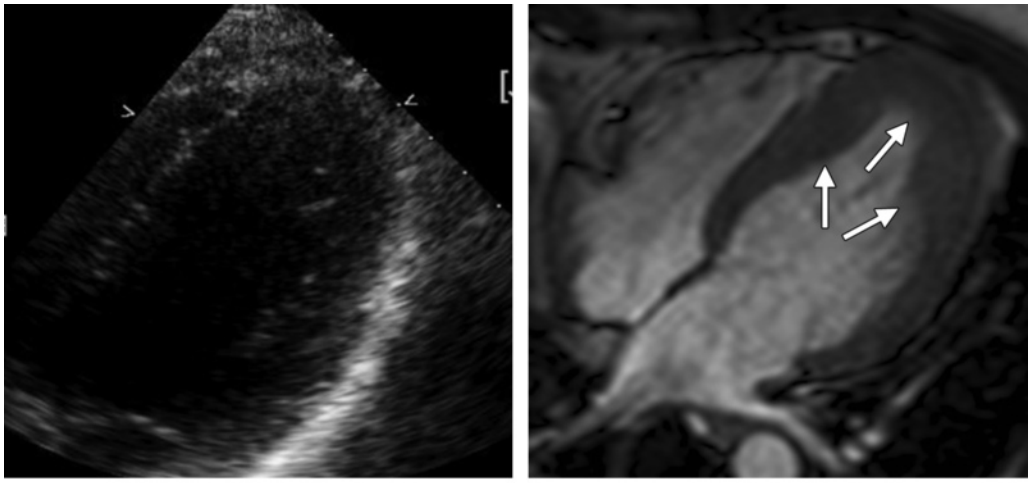

a. b.

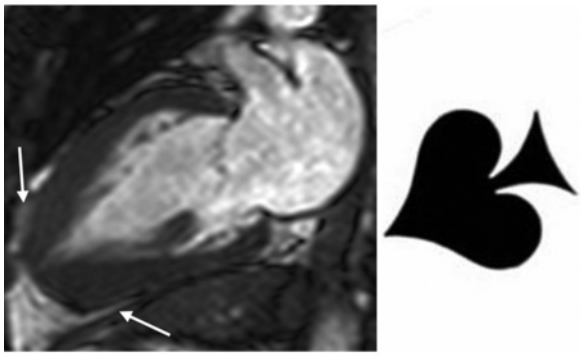

c.

Apical HCM

Apical HCM is characterized as myocardial hypertrophy that predominantly involves the apex of the left ventricle. Apical HCM was originally described in individuals of Asian descent but is now being diagnosed increasingly in the Western world (28,29). The reported rate of occurrence of apical HCM varies in the literature, ranging from 25% of all patients with HCM in Japan to fewer than 2% of the patients with HCM in Western countries (18). Unlike typical HCM, apical HCM *(a)* shows a predilection for middle-aged men, *(b)* is rarely associated with sudden cardiac death, *(c)* is frequently complicated by hypertension, and *(d)* has a relatively good prognosis (29,30). Apical HCM may show typical electrocardiographic abnormalities in the form of giant negative T waves (31).

Teaching Point

The diagnostic criterion for apical HCM is *(a)* an absolute apical wall thickness of more than 15 mm or *(b)* a ratio of apical to basal LV wall thicknesses of 1.3–1.5 (32,33). With MR imaging and multidetector CT, the characteristic "spadelike" configuration of the LV cavity at end diastole, a configuration that is caused by localized apical hypertrophy, is well appreciated on vertical long-axis views (12,13,32,33) (Fig 5). The LV apex may not be assessed well with echocardiography, which can lead to false-negative interpretations in apical HCM. Hence, cardiac MR imaging is strongly recommended as the optimal imaging modality for evaluation of apical HCM (7,8).

Symmetric HCM (Concentric HCM)

Symmetric HCM, or concentric HCM, is characterized by concentric LV hypertrophy with a small cavity dimension and no evidence of a secondary cause. Symmetric HCM is known to occur in as many as 42% of the cases of HCM (17) (Fig 6). This entity should be differentiated from other causes of symmetric increased thickness of

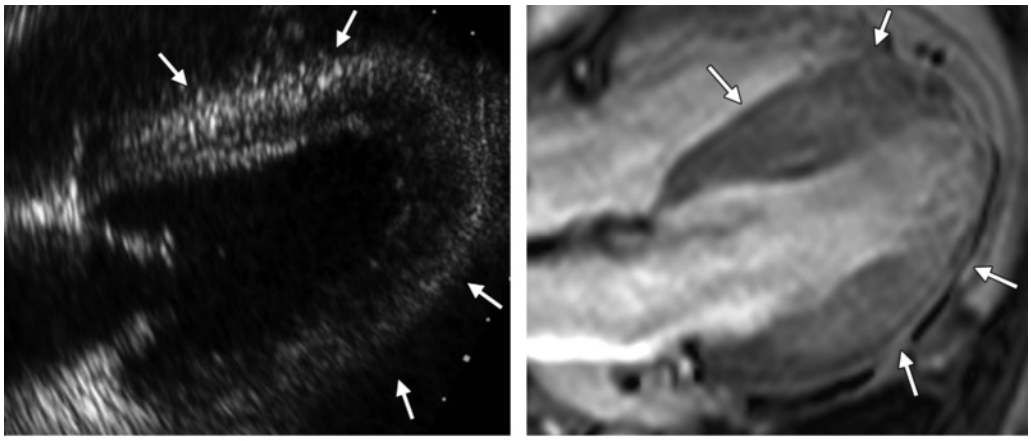

Figure 6. Symmetric HCM (concentric HCM) in a 58-year-old woman with recurrent ventricular tachycardia. **(a)** Four-chamber transthoracic echocardiogram shows borderline LV wall thickening (arrows) of about 14 mm (maximal thickness); differentiation between compensatory hypertrophy and concentric HCM is difficult. **(b)** Four-chamber steady-state free precession cine MR image, however, clearly shows concentric hypertrophy of the entire LV wall (arrows), with a thickness of more than 15 mm at end diastole.

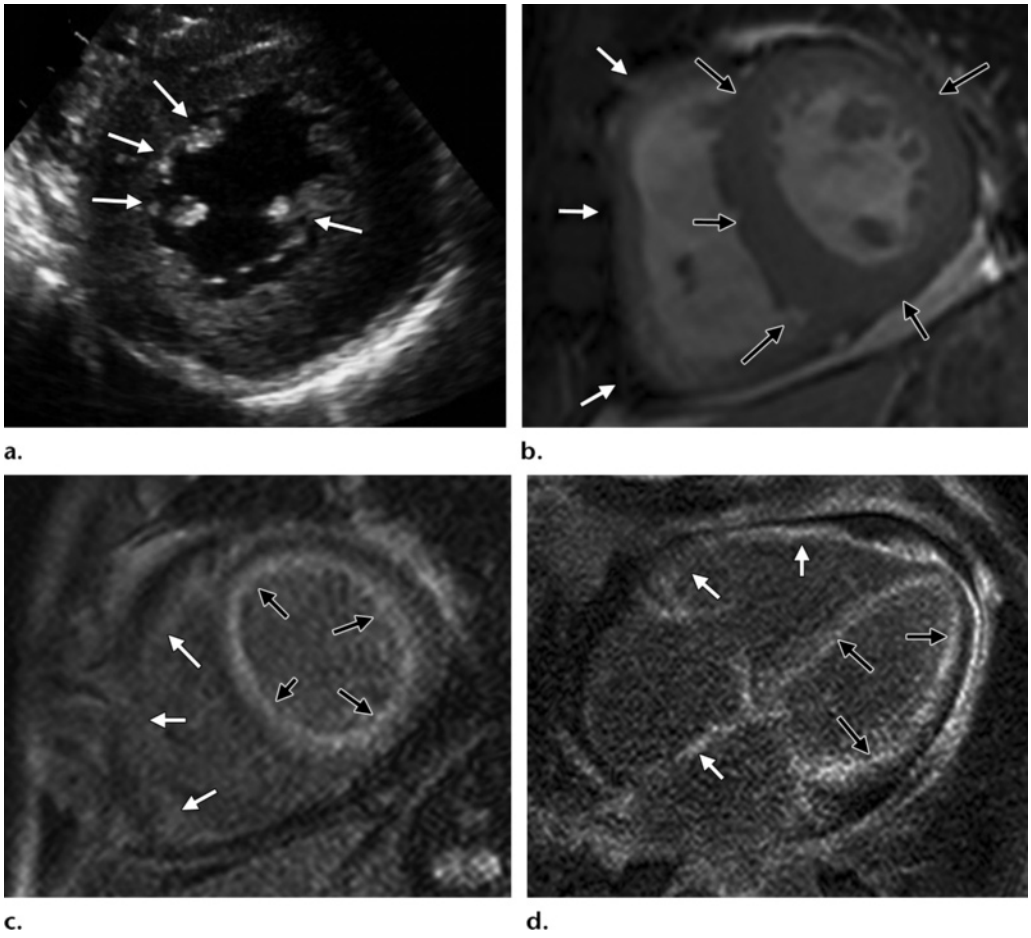

Figure 7. Cardiac amyloidosis in a 58-year-old man with dyspnea. **(a)** Short-axis transthoracic echocardiogram shows concentric LV hypertrophy, with hyperechoic granular sparkling (arrows) of the ventricular wall. **(b)** Short-axis steady-state free precession cine MR image clearly shows increased thickness of the LV wall (black arrows), as well as thickening of the right atrial free wall (white arrows) by more than 6 mm. **(c, d)** Short-axis **(c)** and four-chamber **(d)** DE MR images show the typical global and subendocardial enhancement in the left ventricle (black arrows), the right ventricle (white arrows), and the interatrial septum (single white arrow at bottom in **d**).

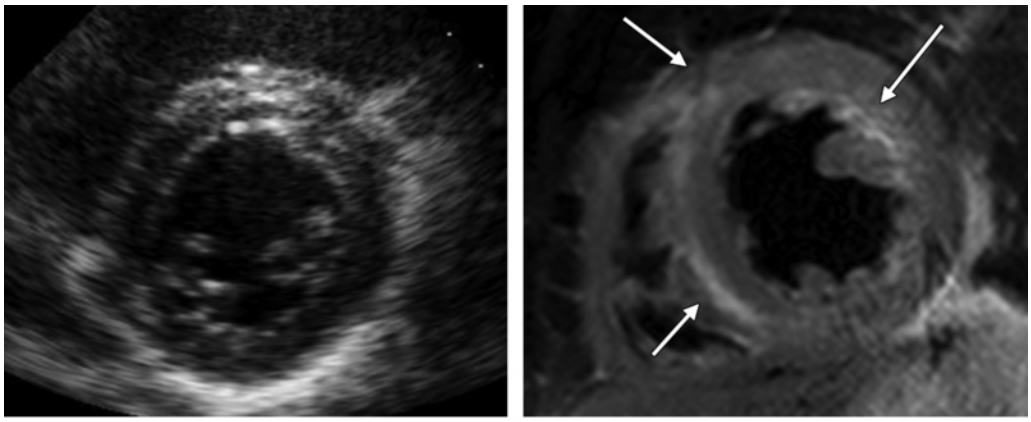

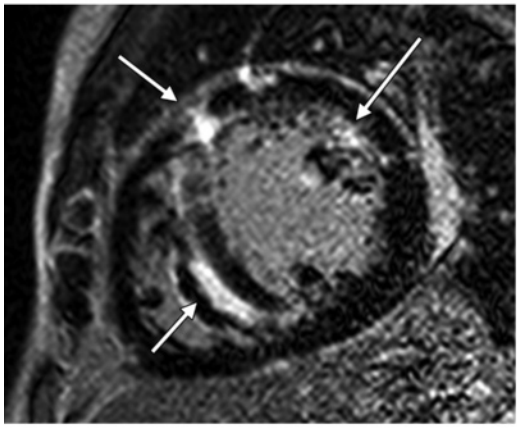

Figure 8. Cardiac sarcoidosis in a 54-year-old woman with palpitations. **(a)** Short-axis transthoracic echocardiogram shows nonspecific borderline LV wall hypertrophy. **(b, c)** Short-axis T2-weighted **(b)** and DE **(c)** MR images demonstrate nodular or patchy increased signal intensity, which involves the septum and the LV wall (arrows), whereas the right ventricular area has no involvement with sarcoidosis.

the LV wall, including athlete's heart, amyloidosis, sarcoidosis, Fabry disease, and the secondary adaptive pattern of LV hypertrophy that is due to hypertension or aortic stenosis, because the treatment strategies are different (34). Cardiac MR imaging is known to play an important role in differentiating other causes of myocardial hypertrophy from HCM because of the unique ability of DE MR imaging to be used to characterize different enhancement patterns in diseased myocardium (10,34).

In cardiac amyloidosis, the amyloid protein is deposited in the myocardium, which leads to diastolic dysfunction that progresses to restrictive cardiomyopathy. Because amyloidosis is a systemic process, involvement of all four chambers is common; thus, an increase in the thickness of the interatrial septum and right atrial free wall by more than 6 mm has been shown to be a specific finding for cardiac amyloidosis (35). Through the use of DE MR imaging, a distinct pattern of late enhancement, which was distributed over the entire subendocardial circumference, has been shown to have high specificity and sensitivity for cardiac amyloidosis (36) (Fig 7).

Sarcoidosis is a noncaseating granulomatous disease that infiltrates any area of the body, but most of the morbidity and mortality are due to invasion of the cardiac system. MR imaging shows nodular or patchy increased signal intensity on both T2-weighted and DE images because of the edema associated with inflammation, which often involves the septum (more particularly, the basal portion) and the LV wall, whereas papillary and right ventricular infiltration are rarely noted (37) (Fig 8).

Athlete's heart refers to morphologic changes in the heart, including increases in LV mass, LV diastolic cavity dimension, and wall thickness, in athletes who train with vigorous physical activity (38). For the ratio of the diastolic wall thickness to the LV end-diastolic volume corrected to body surface area, a value of less than 0.15 mm/m^2/mL has been shown to be useful in differentiating athlete's heart from all other pathologic causes of hypertrophy, with a reported sensitivity of 80% and a specificity of 99% (39). With MR imaging, various geometric indexes, including the diastolic wall thickness, LV end-diastolic volume, and ejection fraction, were correctly obtained for the identification of athlete's heart. Another feature of the cardiac remodeling identified in athletes is the lack of areas of delayed hyperenhancement within the LV myocardium at DE MR imaging (18).

Figure 9. Midventricular HCM in a 56-year-old man with dyspnea. Four-chamber transthoracic echocardiogram **(a)** and multidetector CT image **(b)** show LV hypertrophy predominantly in the middle third of the LV wall (arrows), which is assumed to be a dumbbell configuration. However, with echocardiography, the apex (∗ in **a**) is not clearly depicted because of the limited acoustic window, whereas multidetector CT clearly shows the apical border (∗ in **b**).

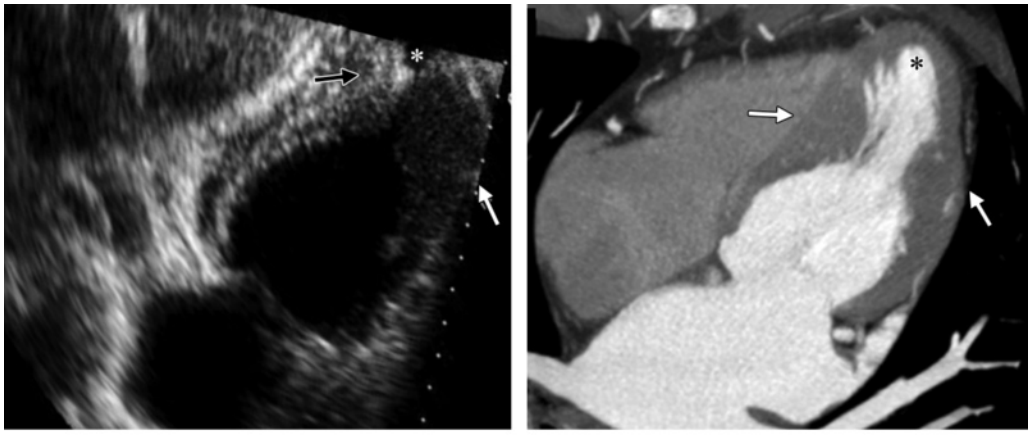

Figure 10. Masslike HCM in a 76-year-old woman with chest discomfort but normal findings at echocardiography. **(a)** Short-axis multidetector CT image shows a masslike bulging contour at apical anterolateral wall (arrows), which was missed at echocardiography. **(b)** Short-axis DE MR image shows focal patchy enhancement within a masslike lesion (arrow).

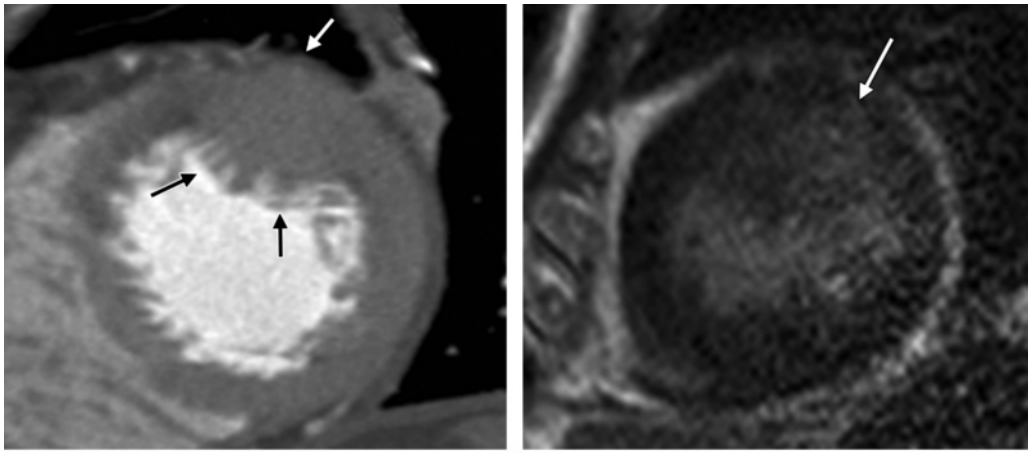

Fabry disease is a rare X-linked autosomal recessive metabolic storage disorder caused by a lack of lysosomal α-galactosidase A. At MR imaging, the LV wall is seen to be concentrically thickened, and delayed hyperenhancement is typically seen midwall and has been reported in the basal inferolateral segment in 12 (92%) of 13 patients at DE MR imaging (40).

In patients with hypertension or aortic stenosis, the LV wall shows compensatory hypertrophy with a more concentric pattern because of adaptation caused by pressure overload. However, differentiation between compensatory hypertrophy and HCM is sometimes difficult (41). In comparison with the patients with HCM, the patients with compensatory hypertrophy usually have systolic function in the normal range, rather than hyperdynamic systolic function, and their LV wall rarely exceeds 15 mm in maximal thickness and is rarely enhanced at DE MR imaging (42).

Midventricular HCM

Midventricular HCM is a rare variant of asymmetric HCM and is characterized by hypertrophy occurring predominantly in the middle third of the LV wall and by systolic apposition of the mid-

Figure 11. Noncontiguous HCM in a 38-year-old man with electrocardiographic abnormalities of ST elevation in leads V_2 through V_4 and T-wave inversion in leads V_4 through V_6. **(a)** Short-axis transthoracic echocardiogram does not depict hypertrophic myocardium or wall motion abnormality because of the poor acoustic window. **(b)** Short-axis multidetector CT image, however, shows noncontiguous LV hypertrophy of the anteroseptal wall and the inferoseptal wall (arrows), separated by septal areas of normal LV wall thickness (*). **(c)** Short-axis DE MR image shows multifocal patchy enhancement of the hypertrophic anteroseptal and inferoseptal walls (arrows), along with preserved septal wall of normal thickness (*).

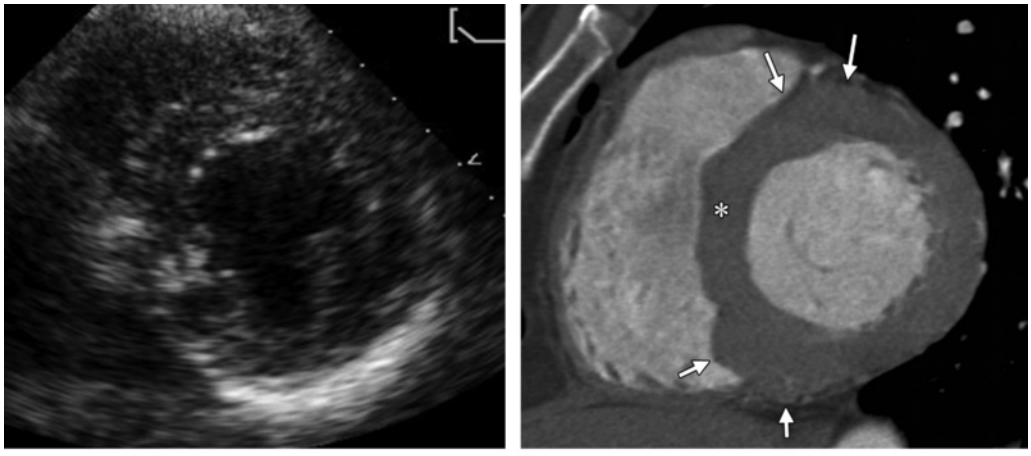

a. b.

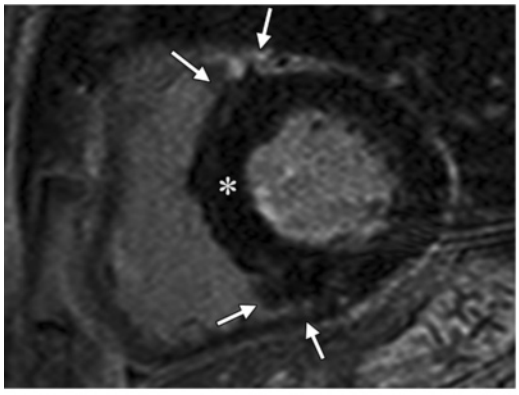

c.

ventricular wall (17,18). Midventricular HCM may be associated with an apical aneurysm caused by increased systolic pressures in the apex from midventricular obstruction. MR imaging and multidetector CT well demonstrate the characteristic "dumbbell" configuration of the LV cavity with marked muscular midcavity systolic constriction (17) (Fig 9). The importance of this variant is its association with ventricular arrhythmia, myocardial necrosis, and systemic embolism (43).

Masslike HCM

Masslike HCM manifests as a masslike hypertrophy because of the focal segmental location of the myocardial disarray and fibrosis (18), which may be differentiated from neoplastic masses. MR imaging with spin-echo pulse sequences, first-pass perfusion, and the DE technique helps to differentiate between the two entities. Masslike HCM more precisely parallels the homogeneous signal intensity characteristics and perfusion of adjacent normal myocardium, whereas tumors show heterogeneous signal intensity and enhancement and show perfusion characteristics that differ from those of the remainder of the left ventricle (Fig 10). Myocardial tagging with the steady-state free precession technique is also useful in differentiating the masslike HCM from a tumor because of the absence of active contraction in tumors, in comparison with the presence of contractility in HCM (44).

Noncontiguous HCM

In a recent study, Maron et al (9) reported that noncontiguous distribution of segmental areas of LV hypertrophy was found in 42 (13%) of the 333 patients with HCM. The morphologic pattern of noncontiguous HCM consists of hypertrophic segments separated by regions of nonhypertrophic myocardium, a pattern that creates abrupt changes in wall thickness in adjacent portions of the wall and a "lumpy" hypertrophic pattern (9). MR imaging can be used to help provide an accurate diagnosis of noncontiguous HCM; this variant of HCM may be missed or substantially underestimated if only two-dimensional echocardiography is used (9) (Fig 11).

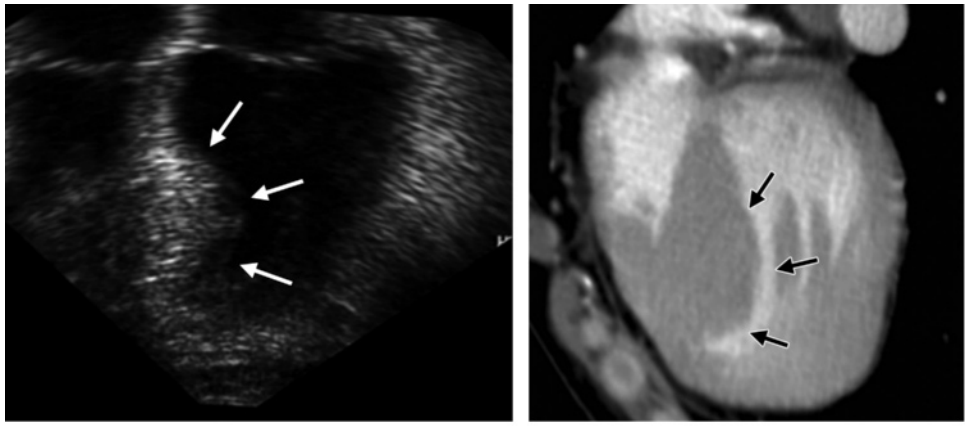

a. b.

Figure 12. Reverse-curve HCM in a 28-year-old woman with a family history of HCM. Four-chamber transthoracic echocardiogram **(a)** and multidetector CT image **(b)** show the septal wall hypertrophy with the reversed *S*-type curve of the septal contour (arrows).

Reverse-Curve HCM and Sigmoid HCM

Other specific types of HCM are the reverse-curve type and the sigmoid type, which were classified by septal morphologic subtypes on the basis of echocardiographic long-axis images obtained at end diastole (45) (Fig 12). Reverse-curve HCM is frequently seen in young patients with HCM and has a large tendency to be associated with positive results of the genetic test for myofilament HCM (in 80%); reverse-curve HCM is often associated with a family history of sudden cardiac death, hypertension, and increased LVOT pressure. Sigmoid HCM, which is characterized by an isolated basal septal bulge yielding a sigmoid septal contour, tends to occur in elderly patients, and fewer than 10% of those have positive findings with the same genetic test (45).

Preclinical HCM

Screening of the family members of a patient with HCM is important because the first-degree relatives of such a patient have a 50% chance of being a gene carrier (2). However, disease expression can be heterogeneous and varied, even with the same mutation; hence, follow-up screening may need to be considered every 2–5 years, particularly in young patients (1).

In one previous report (46), an LV crypt, which is defined as a blind pit or *V*-shaped fissure extending into but confined by the myocardium, was identified at cine MR imaging with a high rate of occurrence of 81% (13 of 16 subjects) in HCM mutation carriers who had not yet developed LV hypertrophy. The LV crypt is suggested to be one of the early pathologic alterations of the myocardium that ultimately progress into HCM (42). Srichai et al (47) described the findings from cardiac multidetector CT in 15 patients with 23 incidentally noted LV crypts. Srichai et al (47) suggested that LV crypts are more common than previously thought and are located predominantly at the insertion points of the right ventricle into the left ventricle (Fig 13). The LV crypts might be caused by locally altered loading conditions or myocardial contractility (48).

Therefore, cardiac MR imaging and multidetector CT might be useful screening tools in patients with a normal LV thickness who have symptoms of HCM or in asymptomatic HCM mutation carriers. Although cardiac MR imaging and multidetector CT provide a new method for diagnosing preclinical HCM, more information about its natural history and prognosis is needed (47). In addition, whether hyperenhancement at DE MR imaging can be identified before the development of LV hypertrophy in preclinical patients has not been determined. In a recently published case report, Strijack et al (49) identified a young asymptomatic patient with preclinical HCM who had extensive and diffuse delayed hyperenhancement throughout the left ventricle despite an otherwise structurally normal ventricle with preserved systolic function.

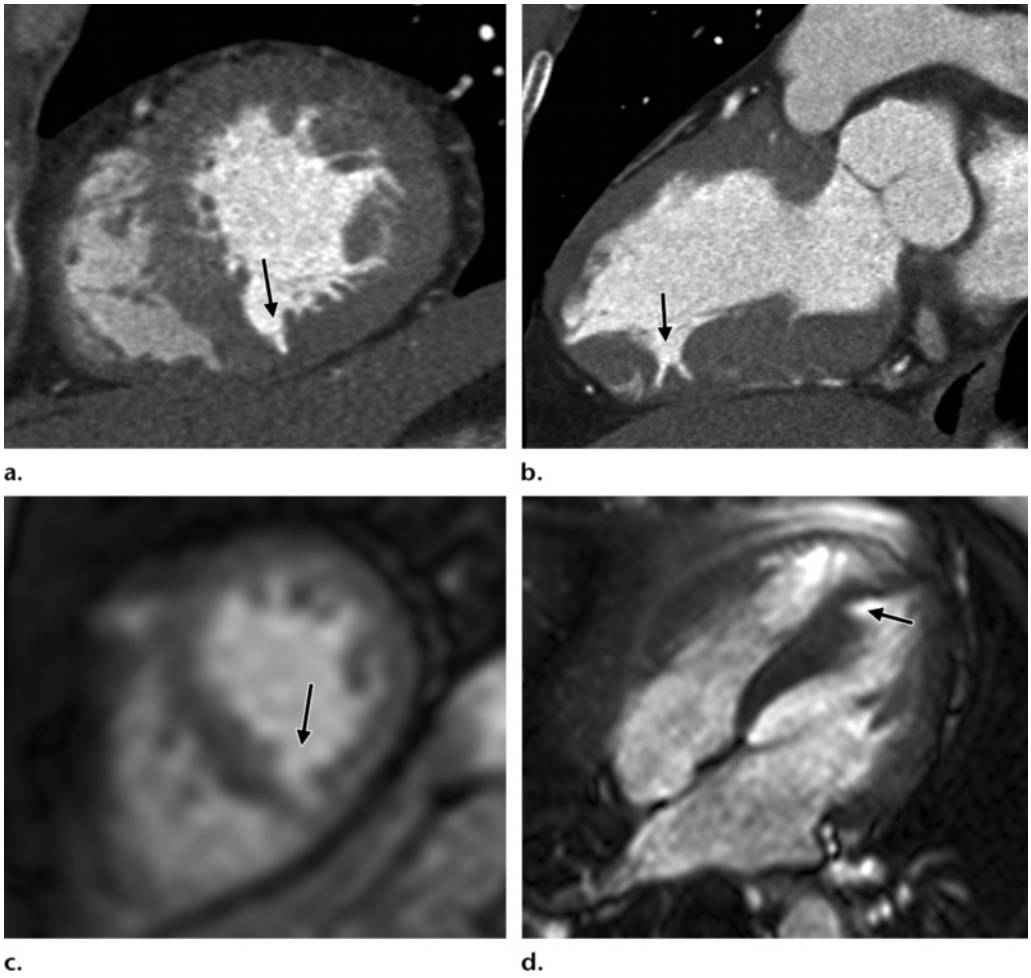

Figure 13. LV crypt in a 52-year-old man with incidentally detected findings. **(a, b)** Short-axis **(a)** and two-chamber **(b)** multidetector CT images show the linear penetration (arrow) of the compact myocardium at the midventricular inferoseptal wall at end diastole. **(c, d)** Short-axis **(c)** and four-chamber **(d)** steady-state free precession cine MR images also show the same findings that were depicted on the multidetector CT images, including the LV crypt (arrow). The crypt closes almost completely during systole.

Risk Stratification of HCM

Sudden cardiac death is the most devastating and unpredictable complication of HCM, and the overall annual mortality rate ranges from less than 1% in asymptomatic patients to 6% in patients with high-risk factors (2). Because sudden cardiac death may occur as the initial manifestation of HCM without reliable warning signs or symptoms, particularly in young patients, the identification of individuals at a high risk for sudden cardiac death among the various manifestations of HCM has become an important challenge. The American College of Cardiology/European Society of Cardiology guidelines (1) indicate the major risk factors for sudden cardiac death as follows: *(a)* cardiac arrest (ventricular fibrillation), *(b)* spontaneous sustained ventricular tachycardia, *(c)* a family history of premature sudden death, *(d)* unexplained syncope, *(e)* LV wall thickness greater than or equal to 30 mm, *(f)* abnormal exercise blood pressure, and *(g)* nonsustained ventricular tachycardia (Holter).

Table 1
Applications of Cardiac Imaging Modalities for Stratification of the Risk of Sudden Cardiac Death in Patients with HCM

Risk Factor	Echocardiography	Multidetector CT	MR Imaging
LV maximal wall thickness of 30 mm or more	+	+	+
Marked LVOT obstruction (LVOT gradient ≥ 30 mm Hg at rest)	+	−	+
LV dilatation and depressed ejection fraction	+	+	+
Fibrosis	−	−	+*
Perfusion defect	−	±	+
Reduced functional reserve flow	±	−	+

Note.—+ = modality can be used to assess the risk factor, − = modality is not useful for assessing the risk factor, ± = modality is available for assessing the risk factor, but the usefulness of the modality is still investigational and is not validated yet.
*Detection at DE MR imaging.

Teaching Point

Among such risk factors, those with potential applications in cardiac imaging for stratification of the risk of sudden cardiac death in patients with HCM are as follows: *(a)* LV maximal wall thickness of 30 mm or more, *(b)* LVOT gradient of 30 mm Hg or more at rest or 50 mm Hg or more with provocation, *(c)* LV dilatation with depressed ejection fraction, *(d)* presence of fibrosis, *(e)* perfusion defect, and *(f)* reduced functional reserve flow (10) (Table 1).

LV Wall Thickness

Maximal LV wall thickness, especially a thickness of 30 mm or more, has been reported as a strong predictor of the risk of sudden death in patients with HCM (50). This relationship of extreme hypertrophy to sudden cardiac death is accentuated in younger patients; it reflects either preferential sudden cardiac death at a young age, structural remodeling with wall thinning, or both (1). With echocardiography, the magnitude of hypertrophy tends to be substantially underestimated in comparison with MR imaging for the assessment of massive LV hypertrophy (wall thickness ≥30 mm) (5,51,52) (Fig 14).

LVOT Obstruction

Historically, the LVOT gradient has been a prominent and quantifiable feature of HCM. Maron et al (53) reported that patients with LVOT obstruction (defined as a basal gradient of ≥30 mm Hg) have an increased risk—more than four times that among patients without obstruction—of sudden cardiac death from HCM or progression to severe congestive symptoms. Kofflard et al (54), who investigated the clinical outcome and risk factors of HCM in a community-based population (not a hospital-based population), also reported that patients with "significant" LVOT obstruction (≥50 mm Hg at rest or with provocation) are susceptible to clinical deterioration in their condition.

LV Dilatation with Depressed Ejection Fraction (Burned-out Phase)

Although most patients with HCM have diastolic dysfunction, a small distinctive subset of patients paradoxically have HCM that evolves into a phase characterized by systolic dysfunction, LV dilatation, and wall thinning (2), which can be demonstrated with MR imaging and multidetector CT. This dilated-hypokinetic evolution of HCM is often called the end-stage or burned-out phase. The clinical course is unfavorable once HCM gets to this phase because it has usually progressed to a heart failure unresponsive to therapy with medications; and, ultimately, heart transplantation remains the only definitive treatment option (55). Therefore, vigilant follow-up and careful risk stratification should be required

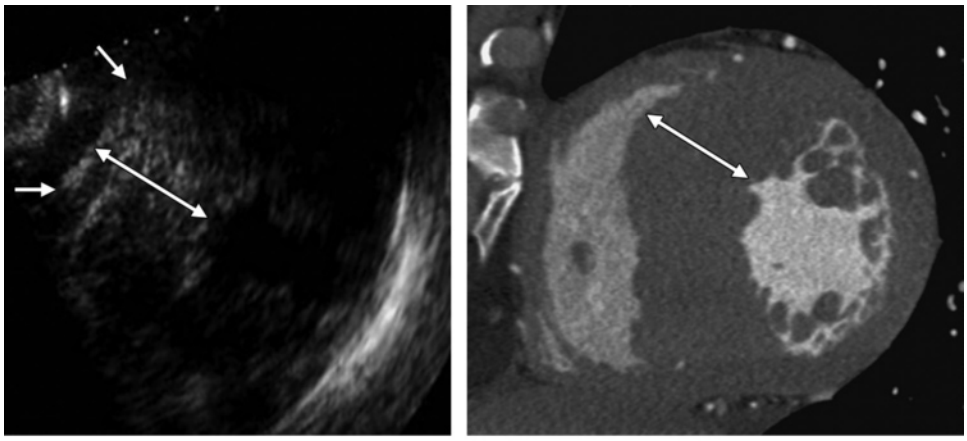

a. b.

Figure 14. Asymmetric (septal) HCM in a 48-year-old man with findings of left bundle branch block at electrocardiography. Short-axis transthoracic echocardiogram **(a)** and multidetector CT image **(b)** show the markedly increased thickness of mainly the apical to the basal septal wall (double-headed arrow). However, the LV thickness is underestimated more with echocardiography (arrows in **a**) than with multidetector CT (about 25 mm in **a**, compared with >32 mm in **b**).

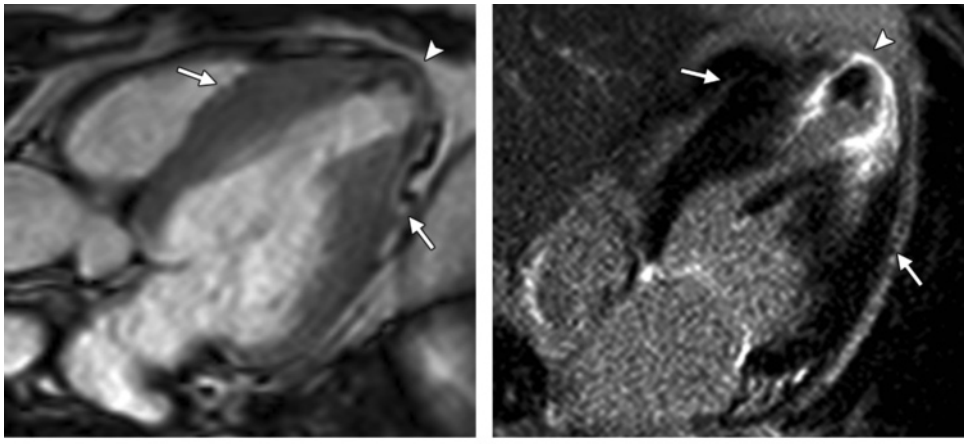

a. b.

Figure 15. Midventricular to apical HCM in the burned-out phase in a 43-year-old woman with severe dyspnea. **(a)** Four-chamber steady-state free precession MR image shows midventricular LV hypertrophy (arrows) with the aneurysmal change at the apex and apical portion (arrowhead) that is due to the progression of HCM into the hypokinetic burned-out phase. **(b)** Two-chamber DE MR image clearly depicts the enhanced thinned apical LV wall (arrows), with a mural thrombus (arrowhead). Global systolic function also decreased because the ejection fraction was 35%.

for timely detection of a transition to the burned-out phase and to permit early treatment before progression to heart failure (56). Such hypokinesia can occur after an acute myocardial infarction, or it can develop gradually without a clinical infarction. Patients with midventricular or apical HCM are at a higher risk of developing segmental or diffuse LV hypokinesia (57,58). MR imaging reveals a thin-walled apical aneurysm showing transmural enhancement that extends into substantial areas of the contiguous interventricular septum and LV free wall (Fig 15). Furthermore,

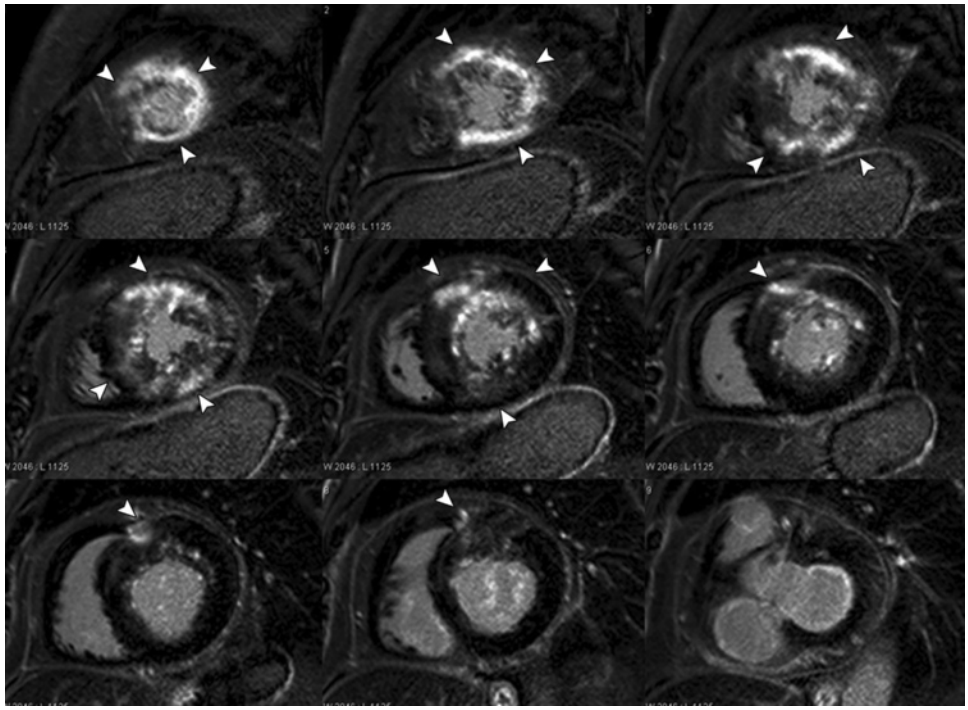

Figure 16. HCM in a 46-year-old man with recurrent ventricular tachycardia. Serial short-axis DE MR images show the patchy enhancement with multiple foci (arrowheads) in the asymmetric hypertrophic apical to basal wall.

thrombus, which is frequently associated with an apical aneurysm, is readily detected at DE MR imaging because thrombus manifests as a low-signal-intensity mass with lack of enhancement.

Presence of Fibrosis

The presence of fibrosis or scarring in HCM can be evaluated with DE MR imaging, which is performed 10–30 minutes after starting the intravenous injection of the gadolinium-based contrast medium (gadolinium chelate); a segmented inversion-recovery sequence is used (59). The extent of fibrosis or scarring has been associated with clinical markers of sudden cardiac death risk and progression to heart failure (60). DE MR imaging relies on the intravenous delivery of a gadolinium chelate to the myocardium; the chelate is a biologically inert tracer that freely distributes in extracellular water but is unable to penetrate the intact cell membrane. In fibrosis and extracellular expansion, there is greater extracellular space for gadolinium accumulation, and the distribution kinetics are slower than in normal myocardium (61).

Teaching Point

At DE MR imaging, hyperenhancement of hypertrophic myocardium is frequently seen in as many as 80% of the patients with HCM; on average, 10% of the overall LV myocardial volume demonstrates hyperenhancement. As opposed to the pattern in patients with coronary artery disease, the pattern of hyperenhancement at DE MR imaging of patients with HCM does not typically correspond to a coronary vascular distribution. Patchy midwall enhancement with multiple foci is the most common form in HCM (9,62) (Fig 16). Delayed hyperenhancement has been correlated with wall thickness (60), regional wall motion abnormalities (63), and the development of ventricular tachyarrhythmia (62,64).

However, Choudhury et al (63) reported that myocardial scarring is common in patients with asymptomatic or mildly symptomatic HCM, and the enhancement of such a benign form is

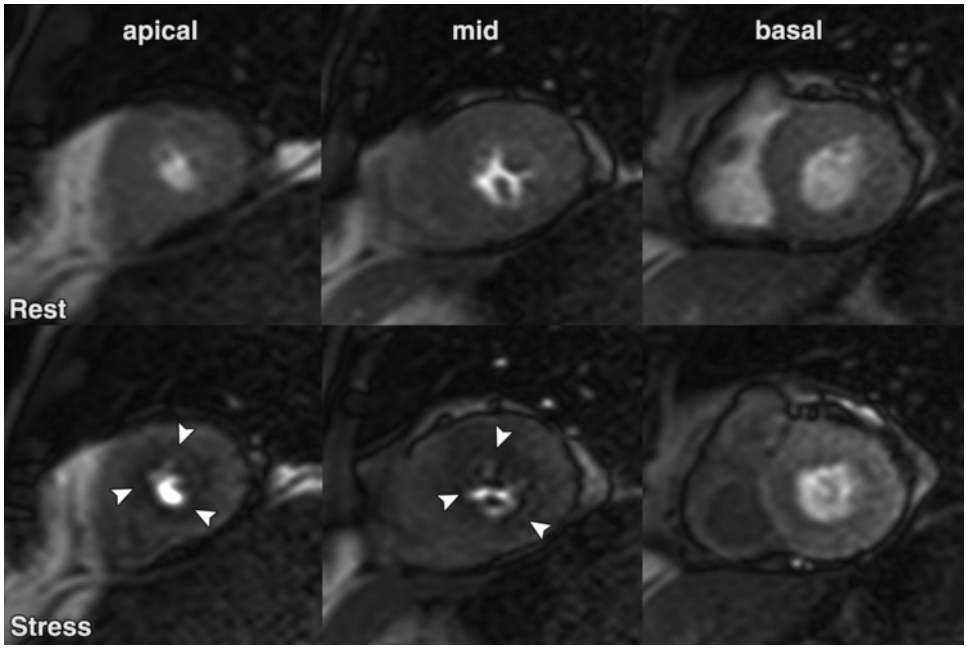

Figure 17. Midventricular to apical HCM in a 67-year-old man with chest discomfort. Short-axis first-pass perfusion MR images obtained with the patient at rest (upper row) and with adenosine-induced stress (lower row) demonstrate a reversible perfusion defect (subendocardial ring of low-signal-intensity enhancement on only the stress perfusion images) at the apical to the midventricular LV wall (arrowheads), a finding that is suggestive of inducible ischemia.

characteristically localized to the junctions of the septum and right ventricular free wall. Whether extreme myocardial scarring is an independent predictor of an adverse prognosis or adds incremental prognostic information to the magnitude of the LV hypertrophy will demand further study.

Perfusion Defect

Myocardial ischemia and reduced myocardial blood flow have been demonstrated in patients with HCM by using thallium perfusion imaging (65) or positron emission tomography (PET) (66). The identification of myocardial ischemia by using PET in patients with HCM is a powerful independent predictor of cardiovascular mortality and may be used to identify patients who are more likely to suffer progressive adverse LV remodeling, including development of the end-stage phase of HCM (9). In this regard, stress perfusion MR imaging now permits accurate qualitative and quantitative assessment of myocardial blood flow at rest and during pharmacologic stress, with superior spatial resolution to that of PET (9). The severity of perfusion impairment in HCM is correlated with the degree of LV hypertrophy (67) (Fig 17).

In patients with HCM who have coexistent epicardial coronary disease, because epicardial coronary disease is one of several etiologic mechanisms that contribute to myocardial ischemia in HCM, it can be difficult to interpret whether the ischemia is caused by the HCM or by the decreased coronary flow reserve. Cardiac multidetector CT can provide useful information for the noninvasive assessment of coexistent epicardial coronary disease in patients with HCM.

Conclusions

Technical advances in cardiac MR imaging and multidetector CT allow the noninvasive assessment of HCM. The relative merits of noninvasive

Table 2
Relative Merits of Each Noninvasive Imaging Modality for the Assessment of HCM

Factor Assessed	Echocardiography*	Multidetector CT	MR Imaging
LV volume	+++	++	++++
LV hypertrophy	+++	++++	++++
Ejection fraction	+++	+++	++++
Regional function	+++	++	++++
LV filling pressure	+++	−	++
PA pressure	+++	−	+++
Dynamic obstruction	+++	+	+++
Mitral regurgitation	+++	−	++
Ischemia/CFR	+	−	++
Monitoring of therapy	+++	+	+++
Tissue characterization	++	+	++++
Preclinical diagnosis	++	+++	+++

Note.—The number of plus signs indicates the relative usefulness of the modality. − = modality is not useful, CFR = coronary flow reserve, PA = pulmonary artery.
*Data in this column are from Nagueh and Mahmarian (10).

imaging with various modalities are summarized in Table 2. Cardiac MR imaging and multidetector CT are capable of providing clinically useful information for the accurate diagnosis of HCM, as well as for the determination of clinical management strategies. In conclusion, radiologists should be familiar with the various findings, as assessed with MR imaging and multidetector CT, and the clinical importance of those findings for the accurate diagnosis and proper management of cases of HCM.

Acknowledgments.—We gratefully acknowledge Goo-Yeong Cho, MD, Seoul National University Bundang Hospital, Seongnam-si, Korea, and Woo Ki Jeon, MD, Vievisnamuh Clinics, Seoul, Korea, for their contributions in performing echocardiographic and MR imaging.

References

1. Maron BJ, McKenna WJ, Danielson GK, et al. American College of Cardiology/European Society of Cardiology clinical expert consensus document on hypertrophic cardiomyopathy: a report of the American College of Cardiology Foundation Task Force on Clinical Expert Consensus Documents and the European Society of Cardiology Committee for Practice Guidelines. J Am Coll Cardiol 2003;42(9):1687–1713.
2. Maron BJ. Hypertrophic cardiomyopathy: a systematic review. JAMA 2002;287(10):1308–1320.
3. Marian AJ, Roberts R. Recent advances in the molecular genetics of hypertrophic cardiomyopathy. Circulation 1995;92(5):1336–1347.
4. Soor GS, Luk A, Ahn E, et al. Hypertrophic cardiomyopathy: current understanding and treatment objectives. J Clin Pathol 2009;62(3):226–235.
5. Rickers C, Wilke NM, Jerosch-Herold M, et al. Utility of cardiac magnetic resonance imaging in the diagnosis of hypertrophic cardiomyopathy. Circulation 2005;112(6):855–861.
6. Prasad K, Atherton J, Smith GC, McKenna WJ, Frenneaux MP, Nihoyannopoulos P. Echocardiographic pitfalls in the diagnosis of hypertrophic cardiomyopathy. Heart 1999;82(suppl 3):III8–III15.
7. Pennell DJ, Sechtem UP, Higgins CB, et al. Clinical indications for cardiovascular magnetic resonance (CMR): Consensus Panel report. Eur Heart J 2004;25(21):1940–1965.
8. Lima JA, Desai MY. Cardiovascular magnetic resonance imaging: current and emerging applications. J Am Coll Cardiol 2004;44(6):1164–1171.
9. Maron MS, Maron BJ, Harrigan C, et al. Hypertrophic cardiomyopathy phenotype revisited after 50 years with cardiovascular magnetic resonance. J Am Coll Cardiol 2009;54(3):220–228.
10. Nagueh SF, Mahmarian JJ. Noninvasive cardiac imaging in patients with hypertrophic cardiomyopathy. J Am Coll Cardiol 2006;48(12):2410–2422.
11. Yoshida M, Takamoto T. Left ventricular hypertrophic patterns and wall motion dynamics in hypertrophic cardiomyopathy: an electron beam computed tomographic study. Intern Med 1997;36(4):263–269.
12. Ghersin E, Lessick J, Litmanovich D, Engel A, Reisner S. Comprehensive multidetector CT assessment of apical hypertrophic cardiomyopathy. Br J Radiol 2006;79(948):e200–e204.

13. Juergens KU, Wessling J, Fallenberg EM, Mönnig G, Wichter T, Fischbach R. Multislice cardiac spiral CT evaluation of atypical hypertrophic cardiomyopathy with a calcified left ventricular thrombus. J Comput Assist Tomogr 2000;24(5):688–690.
14. Williams TJ, Manghat NE, McKay-Ferguson A, Ring NJ, Morgan-Hughes GJ, Roobottom CA. Cardiomyopathy: appearances on ECG-gated 64-detector row computed tomography. Clin Radiol 2008;63(4):464–474.
15. Spirito P, Autore C. Management of hypertrophic cardiomyopathy. BMJ 2006;332(7552):1251–1255.
16. Park JH, Kim YM, Chung JW, Park YB, Han JK, Han MC. MR imaging of hypertrophic cardiomyopathy. Radiology 1992;185(2):441–446.
17. Hughes SE. The pathology of hypertrophic cardiomyopathy. Histopathology 2004;44(5):412–427.
18. Hansen MW, Merchant N. MRI of hypertrophic cardiomyopathy. I. MRI appearances. AJR Am J Roentgenol 2007;189(6):1335–1343.
19. Wigle ED. Cardiomyopathy: the diagnosis of hypertrophic cardiomyopathy. Heart 2001;86(6):709–714.
20. Kansal S, Roitman D, Sheffield LT. Interventricular septal thickness and left ventricular hypertrophy: an echocardiographic study. Circulation 1979;60(5):1058–1065.
21. Elliott P, McKenna WJ. Hypertrophic cardiomyopathy. Lancet 2004;363(9424):1881–1891.
22. Maron MS, Olivotto I, Zenovich AG, et al. Hypertrophic cardiomyopathy is predominantly a disease of left ventricular outflow tract obstruction. Circulation 2006;114(21):2232–2239.
23. Luckie M, Khattar RS. Systolic anterior motion of the mitral valve: beyond hypertrophic cardiomyopathy. Heart 2008;94(11):1383–1385.
24. Halpern EJ. Cardiac morphology and function. In: Clinical cardiac CT: anatomy and function. New York, NY: Thieme, 2008; 166–175.
25. Shah JS, Esteban MT, Thaman R, et al. Prevalence of exercise-induced left ventricular outflow tract obstruction in symptomatic patients with non-obstructive hypertrophic cardiomyopathy. Heart 2008;94(10):1288–1294.
26. White RD, Obuchowski NA, Gunawardena S, et al. Left ventricular outflow tract obstruction in hypertrophic cardiomyopathy: presurgical and postsurgical evaluation by computed tomography magnetic resonance imaging. Am J Card Imaging 1996;10(1):1–13.
27. Amano Y, Takayama M, Amano M, Kumazaki T. MRI of cardiac morphology and function after percutaneous transluminal septal myocardial ablation for hypertrophic obstructive cardiomyopathy. AJR Am J Roentgenol 2004;182(2):523–527.
28. Sakamoto T, Tei C, Murayama M, Ichiyasu H, Hada Y. Giant T wave inversion as a manifestation of asymmetrical apical hypertrophy (AAH) of the left ventricle: echocardiographic and ultrasono-cardiotomographic study. Jpn Heart J 1976;17(5):611–629.
29. Eriksson MJ, Sonnenberg B, Woo A, et al. Long-term outcome in patients with apical hypertrophic cardiomyopathy. J Am Coll Cardiol 2002;39(4):638–645.
30. Webb JG, Sasson Z, Rakowski H, Liu P, Wigle ED. Apical hypertrophic cardiomyopathy: clinical follow-up and diagnostic correlates. J Am Coll Cardiol 1990;15(1):83–90.
31. Yamaguchi H, Ishimura T, Nishiyama S, et al. Hypertrophic nonobstructive cardiomyopathy with giant negative T waves (apical hypertrophy): ventriculographic and echocardiographic features in 30 patients. Am J Cardiol 1979;44(3):401–412.
32. Moon JC, Fisher NG, McKenna WJ, Pennell DJ. Detection of apical hypertrophic cardiomyopathy by cardiovascular magnetic resonance in patients with non-diagnostic echocardiography. Heart 2004;90(6):645–649.
33. Suzuki J, Shimamoto R, Nishikawa J, et al. Morphological onset and early diagnosis in apical hypertrophic cardiomyopathy: a long term analysis with nuclear magnetic resonance imaging. J Am Coll Cardiol 1999;33(1):146–151.
34. Hansen MW, Merchant N. MRI of hypertrophic cardiomyopathy. II. Differential diagnosis, risk stratification, and posttreatment MRI appearances. AJR Am J Roentgenol 2007;189(6):1344–1352.
35. Fattori R, Rocchi G, Celletti F, Bertaccini P, Rapezzi C, Gavelli G. Contribution of magnetic resonance imaging in the differential diagnosis of cardiac amyloidosis and symmetric hypertrophic cardiomyopathy. Am Heart J 1998;136(5):824–830.
36. Vogelsberg H, Mahrholdt H, Deluigi CC, et al. Cardiovascular magnetic resonance in clinically suspected cardiac amyloidosis: noninvasive imaging compared to endomyocardial biopsy. J Am Coll Cardiol 2008;51(10):1022–1030.
37. Vignaux O. Cardiac sarcoidosis: spectrum of MRI features. AJR Am J Roentgenol 2005;184(1):249–254.
38. Maron BJ, Pelliccia A, Spirito P. Cardiac disease in young trained athletes: insights into methods for distinguishing athlete's heart from structural heart disease, with particular emphasis on hypertrophic cardiomyopathy. Circulation 1995;91(5):1596–1601.
39. Petersen SE, Selvanayagam JB, Francis JM, et al. Differentiation of athlete's heart from pathological forms of cardiac hypertrophy by means of geometric indices derived from cardiovascular magnetic resonance. J Cardiovasc Magn Reson 2005;7(3):551–558.
40. Moon JC, Sachdev B, Elkington AG, et al. Gadolinium enhanced cardiovascular magnetic resonance in Anderson-Fabry disease: evidence for a disease specific abnormality of the myocardial interstitium. Eur Heart J 2003;24(23):2151–2155.
41. Kato TS, Noda A, Izawa H, et al. Discrimination of nonobstructive hypertrophic cardiomyopathy from hypertensive left ventricular hypertrophy on the basis of strain rate imaging by tissue Doppler ultrasonography. Circulation 2004;110(25):3808–3814.
42. O'Hanlon R, Assomull RG, Prasad SK. Use of cardiovascular magnetic resonance for diagnosis and management in hypertrophic cardiomyopathy. Curr Cardiol Rep 2007;9(1):51–56.
43. Cooke JC, Cotton JM, Monaghan MJ. Mid-ventricular HOCM with apical asynergy. Heart 2000;83(5):517.
44. Bergey PD, Axel L. Focal hypertrophic cardiomyopathy simulating a mass: MR tagging for correct diagnosis. AJR Am J Roentgenol 2000;174(1):242–244.

45. Binder J, Ommen SR, Gersh BJ, et al. Echocardiography-guided genetic testing in hypertrophic cardiomyopathy: septal morphological features predict the presence of myofilament mutations. Mayo Clin Proc 2006;81(4):459–467.
46. Germans T, Wilde AA, Dijkmans PA, et al. Structural abnormalities of the inferoseptal left ventricular wall detected by cardiac magnetic resonance imaging in carriers of hypertrophic cardiomyopathy mutations. J Am Coll Cardiol 2006;48(12):2518–2523.
47. Srichai MB, Hecht EM, Kim DC, Jacobs JE. Ventricular diverticula on cardiac CT: more common than previously thought. AJR Am J Roentgenol 2007;189(1):204–208.
48. Germans T, Nijveldt R, van Rossum AC. A more detailed view calls for more detailed definition: description of cardiac morphology with high-resolution CT and MRI. AJR Am J Roentgenol 2008;190(2):W169.
49. Strijack B, Ariyarajah V, Soni R, et al. Late gadolinium enhancement cardiovascular magnetic resonance in genotyped hypertrophic cardiomyopathy with normal phenotype. J Cardiovasc Magn Reson 2008;10(1):58.
50. Spirito P, Bellone P, Harris KM, Bernabo P, Bruzzi P, Maron BJ. Magnitude of left ventricular hypertrophy and risk of sudden death in hypertrophic cardiomyopathy. N Engl J Med 2000;342(24):1778–1785.
51. Grothues F, Smith GC, Moon JC, et al. Comparison of interstudy reproducibility of cardiovascular magnetic resonance with two-dimensional echocardiography in normal subjects and in patients with heart failure or left ventricular hypertrophy. Am J Cardiol 2002;90(1):29–34.
52. Devlin AM, Moore NR, Ostman-Smith I. A comparison of MRI and echocardiography in hypertrophic cardiomyopathy. Br J Radiol 1999;72(855):258–264.
53. Maron MS, Olivotto I, Betocchi S, et al. Effect of left ventricular outflow tract obstruction on clinical outcome in hypertrophic cardiomyopathy. N Engl J Med 2003;348(4):295–303.
54. Kofflard MJ, Ten Cate FJ, van der Lee C, van Domburg RT. Hypertrophic cardiomyopathy in a large community-based population: clinical outcome and identification of risk factors for sudden cardiac death and clinical deterioration. J Am Coll Cardiol 2003;41(6):987–993.
55. Biagini E, Coccolo F, Ferlito M, et al. Dilated-hypokinetic evolution of hypertrophic cardiomyopathy: prevalence, incidence, risk factors, and prognostic implications in pediatric and adult patients. J Am Coll Cardiol 2005;46(8):1543–1550.
56. Harris KM, Spirito P, Maron MS, et al. Prevalence, clinical profile, and significance of left ventricular remodeling in the end-stage phase of hypertrophic cardiomyopathy. Circulation 2006;114(3):216–225.
57. Fighali S, Krajcer Z, Edelman S, Leachman RD. Progression of hypertrophic cardiomyopathy into a hypokinetic left ventricle: higher incidence in patients with midventricular obstruction. J Am Coll Cardiol 1987;9(2):288–294.
58. Matsubara K, Nakamura T, Kuribayashi T, Azuma A, Nakagawa M. Sustained cavity obliteration and apical aneurysm formation in apical hypertrophic cardiomyopathy. J Am Coll Cardiol 2003;42(2):288–295.
59. Moon JC, Reed E, Sheppard MN, et al. The histologic basis of late gadolinium enhancement cardiovascular magnetic resonance in hypertrophic cardiomyopathy. J Am Coll Cardiol 2004;43(12):2260–2264.
60. Moon JC, McKenna WJ, McCrohon JA, Elliott PM, Smith GC, Pennell DJ. Toward clinical risk assessment in hypertrophic cardiomyopathy with gadolinium cardiovascular magnetic resonance. J Am Coll Cardiol 2003;41(9):1561–1567.
61. Kim RJ, Chen EL, Lima JA, Judd RM. Myocardial Gd-DTPA kinetics determine MRI contrast enhancement and reflect the extent and severity of myocardial injury after acute reperfused infarction. Circulation 1996;94(12):3318–3326.
62. Teraoka K, Hirano M, Ookubo H, et al. Delayed contrast enhancement of MRI in hypertrophic cardiomyopathy. Magn Reson Imaging 2004;22(2):155–161.
63. Choudhury L, Mahrholdt H, Wagner A, et al. Myocardial scarring in asymptomatic or mildly symptomatic patients with hypertrophic cardiomyopathy. J Am Coll Cardiol 2002;40(12):2156–2164.
64. Kwon DH, Smedira NG, Rodriguez ER, et al. Cardiac magnetic resonance detection of myocardial scarring in hypertrophic cardiomyopathy: correlation with histopathology and prevalence of ventricular tachycardia. J Am Coll Cardiol 2009;54(3):242–249.
65. O'Gara PT, Bonow RO, Maron BJ, et al. Myocardial perfusion abnormalities in patients with hypertrophic cardiomyopathy: assessment with thallium-201 emission computed tomography. Circulation 1987;76(6):1214–1223.
66. Camici P, Chiriatti G, Lorenzoni R, et al. Coronary vasodilation is impaired in both hypertrophied and nonhypertrophied myocardium of patients with hypertrophic cardiomyopathy: a study with nitrogen-13 ammonia and positron emission tomography. J Am Coll Cardiol 1991;17(4):879–886.
67. Sipola P, Lauerma K, Husso-Saastamoinen M, et al. First-pass MR imaging in the assessment of perfusion impairment in patients with hypertrophic cardiomyopathy and the Asp175Asn mutation of the α-tropomyosin gene. Radiology 2003;226(1):129–137.

Hypertrophic Cardiomyopathy: Assessment with MR Imaging and Multidetector CT

Eun Ju Chun, MD • Sang Il Choi, MD • Kwang Nam Jin, MD • Hyon Joo Kwag, MD • Young Jin Kim, MD • Byoung Wook Choi, MD • Whal Lee, MD • Jae Hyung Park, MD

RadioGraphics 2010; 30:1309–1328 • **Published online** 10.1148/rg.305095074 • **Content Codes:** CA CT MR

Page 1310
Echocardiography is an operator-dependent technique. It is influenced by the acoustic window and is sometimes unable to definitively depict the endocardial border, especially the anterolateral free wall of the left ventricle in the parasternal short-axis view and the apex (2,6).

Page 1310
In a clinical setting for evaluation of HCM, although echocardiography is the simplest imaging technique to use for screening, cardiac MR imaging should be considered as the reference standard for establishing a diagnosis of HCM when the results from echocardiography are inconclusive or are suspected of being false-negative findings. Moreover, cardiac MR imaging is strongly recommended as a powerful imaging modality for differentiating HCM from other cardiomyopathies in the differential diagnosis, as well as for risk stratification of HCM in selected patients. In comparison, cardiac multidetector CT is certainly less useful for the assessment of HCM currently because multidetector CT involves radiation exposure and contrast medium–related problems and provides less information (ie, hemodynamic information, tissue characterization such as fibrosis) than MR imaging does. Although MR imaging and echocardiography may be the imaging modalities of choice in most cases of HCM, multidetector CT would be more appropriate in those cases for which there are specific requests to exclude coronary artery disease and in those cases with contraindications for MR imaging, such as a pacemaker (14).

Page 1315 (Figure on page 1315)
The diagnostic criterion for apical HCM is *(a)* an absolute apical wall thickness of more than 15 mm or *(b)* a ratio of apical to basal LV wall thicknesses of 1.3–1.5 (32,33). With MR imaging and multidetector CT, the characteristic "spadelike" configuration of the LV cavity at end diastole, a configuration that is caused by localized apical hypertrophy, is well appreciated on vertical long-axis views (12,13,32,33) (Fig 5).

Page 1322 (Table on page 1322)
Among such risk factors, those with potential applications in cardiac imaging for stratification of the risk of sudden cardiac death in patients with HCM are as follows: *(a)* LV maximal wall thickness of 30 mm or more, *(b)* LVOT gradient of 30 mm Hg or more at rest or 50 mm Hg or more with provocation, *(c)* LV dilatation with depressed ejection fraction, *(d)* presence of fibrosis, *(e)* perfusion defect, and *(f)* reduced functional reserve flow (10) (Table 1).

Page 1324
At DE MR imaging, hyperenhancement of hypertrophic myocardium is frequently seen in as many as 80% of the patients with HCM; on average, 10% of the overall LV myocardial volume demonstrates hyperenhancement.